Increased Heating Efficiency and Selective Thermal Ablation of Malignant Tissue with DNA-Encased Multiwalled Carbon Nanotubes

Supratim Ghosh,[†,‡] Samrat Dutta,[¶] Evan Gomes,[†] David Carroll,[¶,#] Ralph D'Agostino, Jr.,[§] John Olson,[⊥] Martin Guthold,[¶] and William H. Gmeiner[†,‡,*]

[†]Department of Cancer Biology, [‡]Program in Molecular Genetics, [§]Department of Biostatistical Sciences and [⊥]Center for Biomolecular Imaging, Wake Forest University School of Medicine, Winston-Salem, North Carolina 27157 and [¶]Department of Physics, and [#]Center for Nanotechnology and Nanomaterials, Wake Forest University, Winston-Salem, North Carolina 27109

ABSTRACT Nanoparticles, including multiwalled carbon nanotubes (MWNTs), strongly absorb near-infrared (nIR) radiation and efficiently convert absorbed energy to released heat which can be used for localized hyperthermia applications. We demonstrate for the first time that DNA-encasement increases heat emission following nIR irradiation of MWNTs, and DNA-encased MWNTs can be used to safely eradicate a tumor mass *in vivo*. Upon irradiation of DNA-encased MWNTs, heat is generated with a linear dependence on irradiation time and laser power. DNA-encasement resulted in a 3-fold reduction in the concentration of MWNTs required to impart a 10 °C temperature increase in bulk solution temperature. A single treatment consisting of intratumoral injection of MWNTs (100 μL of a 500 μg/mL solution) followed by laser irradiation at 1064 nm, 2.5 W/cm^2 completely eradicated PC3 xenograft tumors in 8/8 (100%) of nude mice. Tumors that received only MWNT injection or laser irradiation showed growth rates indistinguishable from nontreated control tumors. Nonmalignant tissues displayed no long-term damage from treatment. The results demonstrate that DNA-encased MWNTs are more efficient at converting nIR irradiation into heat compared to nonencased MWNTs and that DNA-encased MWNTs can be used safely and effectively for the selective thermal ablation of malignant tissue *in vivo*.

KEYWORDS: nanotechnology · photothermal therapy · DNA · hyperthermia · near-infrared

The selective thermal ablation of malignant tissue is an important objective in cancer research and offers a viable alternative treatment option when surgical resection is not possible. Modalities such as radiofrequency ablation (RFA) have been shown to be efficacious for treatment of various malignancies including liver, lung, and prostate tumors.[1,2] Cell death is induced by irreversible protein denaturation or membrane damage at temperatures above 40 °C.[3,4] While RFA and other thermal ablative strategies such as ultrasound or microwave treatment[5] offer a less invasive alternative to surgery, these techniques have neither inherent specificity for malignant cells nor any potential to be utilized in a molecularly targeted approach. Thus, the development of novel approaches for the selective sensitization of malignant cells to irradiation is necessary to realize the potential of this methodology.

Various nanoparticles including single-walled carbon nanotubes (SWNTs)[6,7] and gold nanoparticles[8] have been shown to be efficient transducers of near-infrared (nIR) irradiation to generate heat that is sufficient to cause cell death. In the case of SWNTs and multiwalled carbon nanotubes (MWNTs), the mechanism of heat generation involves excitation of optical transitions with relaxation resulting in enhanced vibrational modes in the carbon lattice that cause solution heating.[9] In principle, these nanoparticles can be conjugated with aptamers[10] or antibodies[11] and selectively delivered to malignant cells *in vivo* permitting thermal ablation to be used in a molecularly targeted fashion. In practice, issues relating to the aqueous solubility, biocompatibility, and toxicology of nanoparticles must be addressed prior to successfully translating this approach into the clinic.

Although less well-studied than SWNTs, MWNTs are potentially of great use for the selective thermal ablation of malignant cells as a consequence of the efficient conversion of nIR irradiation into heat by this material which greatly exceeds that of a graphite control.[12] MWNTs are composed of concentric SWNTs and like SWNTs the hydrophobic outer surface must be modified with amphiphilic materials[13] to confer sufficient aqueous solubility for *in vivo* applications. DNA has been utilized to confer

*Address correspondenc to bgmeiner@wfubmc.edu.

Received for review April 10, 2009 and accepted July 28, 2009.

Published online August 5, 2009.
10.1021/nn900368b CCC: $40.75

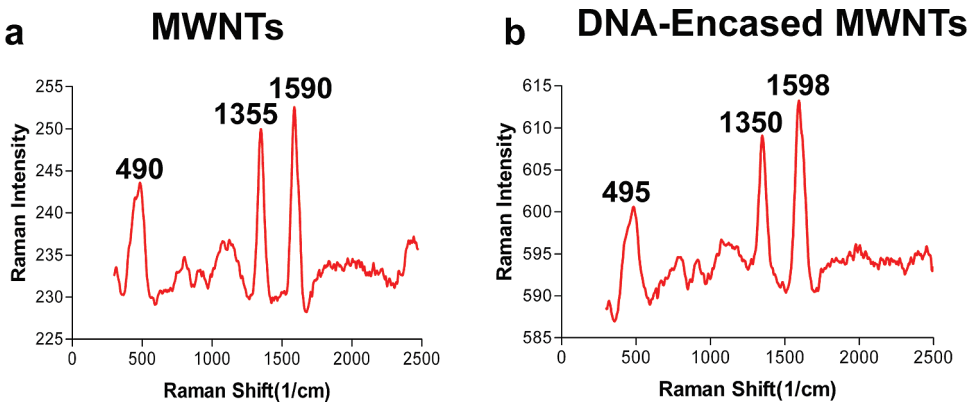

Figure 1. (a) Raman spectrum for non-DNA-encased MWNTs showing the absorbance for the radial breathing mode (RBM) as well as for the D and G-bands; (b) Raman spectra for the DNA-encased MWNTs.

aqueous solubility to SWNTs[14,15] with the hydrophobic nucleobases interacting with the aromatic structure of the SWNTs through $\pi-\pi$ stacking[16] while the deoxyribose sugars and phosphodiester backbone of DNA provide the hydrophilicity necessary for aqueous solubility of DNA-encased SWNTs. Several studies have demonstrated a sequence- and length-dependence to the interaction of SWNTs with DNA with alternating dG-dT copolymers being among the most preferred sequences.[17] The interaction of MWNTs with DNA is less well-studied and MWNTs have larger diameters than SWNTs and thus present a surface with a larger radius of curvature that may interact differently with DNA than that of SWNTs.

The present study was undertaken to establish the feasibility of conferring aqueous solubility to MWNTs using DNA and to investigate to what extent DNA-encased MWNTs are useful for thermal ablation of malignant tissue. The relative efficiency of conversion of nIR irradiation into heat for DNA-encased MWNTs relative to non-DNA-encased MWNTs and other materials is an important consideration for identifying which type of nanomaterial is best-suited for *in vivo* thermal ablation approaches.[12] We have undertaken an analysis of the time-, power-, and concentration-dependence of heat generation from DNA-encased MWNTs. We demonstrate that DNA-encased MWNTs produce larger amounts of heat than non-DNA-encased MWNTs when irradiated under identical conditions indicating that DNA-encasement increases the utility of MWNTs for thermal ablative applications. Further, we demonstrate for the first time that DNA-encased MWNTs efficiently eradicate tumor xenografts *in vivo* in a mouse model of human cancer. Complete tumor eradication was achieved with a single treatment under conditions that resulted in no injury or damage to normal tissues. These findings demonstrate that DNA-encased MWNTs may be useful for development of molecularly targeted nanoparticles for selective thermal ablation of malignant tissue in humans.

RESULTS

Spectral Properties of DNA-Encased MWNTs. Raman spectra of MWNTs and DNA-encased MWNTs were compared to evaluate how DNA-encasement altered the vibrational modes of MWNTs. DNA-encased MWNTs displayed D and G bands that are characteristic of all graphitic materials (Figure 1a,b). The disorder-induced D band detected at 1355 cm^{-1} for the non-DNA-encased MWNTs was detected at 1350 cm^{-1} for the DNA-encased MWNTs. Alterations in D-band frequency and intensity have been attributed previously to charge transfer between DNA nucleobases and NTs;[18] however, no significant change in Raman frequency or intensity was observed in the present study. The radial breathing mode (RBM) was observed for both the DNA-encased MWNT sample and the non-DNA-encased MWNTs at $\sim$492 cm^{-1} indicating the diameter for the innermost carbon nanotube in the MWNT is approximately 0.45 nm.[19] Analysis of AFM and SEM images revealed that the diameter for the outermost carbon nanotube was $>$40 nm (see following section) consistent with MWNTs comprising multiple concentric layers, as expected.

Imaging Reveals DNA-Encased MWNTs Are Dispersed. AFM and SEM images of DNA-encased MWNTs were obtained in order to assess to what extent aqueous solutions of DNA-encased MWNTs were monodispersed and to assess the size distribution for MWNTs in DNA-encased samples. Figure 2a shows a typical SEM image of non-DNA-encased MWNTs while DNA-encased MWNTs are shown in Figure 2b. Non-DNA-encased MWNTs form aggregates while samples of DNA-encased MWNTs are well dispersed, with mainly single nanotubes. Regions of thickening of the MWNTs consistent with DNA binding were detected in AFM images for DNA-encased MWNTS. The presence of DNA on the MWNTs was verified by fluorescence quenching experiments (Supporting Information Figure S1).

The AFM images (Figure 2c,d) display comparable physical properties as those observed in the SEM image (Figure 2b). It can also be seen that the tubes have a range of lengths and diameters, and that most of them are curved. Continuous variations in NT curvature have been attributed to elasticity while bends in MWNT structures may be caused by topological defects.[20] A more detailed analysis of nanotube morphology is shown in Figure 2e,f. The DNA-encased MWNTs used in these studies had an average diameter of 49 nm, an average length of 571 nm, and an average aspect ratio (length/diameter) of 13. Analysis of the aspect

ratio distribution for the DNA-encased MWNTs and a dot-plot of the length *vs* diameter are included in Supporting Information Figure S2.

Enhanced Solution Heating by DNA-Encased MWNTs. The extent of heating for aqueous solutions of DNA-encased MWNTs was evaluated to determine if encasing the MWNTs in DNA altered the heating efficiency of MWNTs. Aqueous solutions of DNA-encased MWNTs or MWNTs that had not been DNA-encased were irradiated at 1064 nm using a quasi-CW-YAG nIR laser system. Sample heating was evaluated for a range of MWNT concentrations (1−100 μg/mL) at three different power levels (2, 3, 4 W) and for times ranging from 25−70 s. Representative graphs displaying the concentration-dependence and time-dependence of solution heating are displayed in Figure 3.

DNA-encasement of MWNTs significantly reduced the MWNT concentration required for biologically relevant heating. For example, while an MWNT concentration of 30 μg/mL is required for a 5 °C temperature increase upon 3 W nIR irradiation for 25 s, a similar temperature increase with these same irradiation conditions was achieved with DNA-encased MWNTs at a concentration of 15 μg/mL (Figure 3a,b). Similarly, an MWNT concentration of 24 μg/mL is required for a 10 °C temperature increase upon nIR irradiation for 70 s (3 W) while DNA-encased MWNTs achieved this same temperature increase with only 8 μg/mL under identical conditions (Figure 3c,d). Thus, DNA-encasement increases heat production 2- to 3-fold relative to non-DNA-encased MWNTs (Figure 3 and Supporting Information Figure S3). Importantly, DNA-encased MWNTs can achieve biologically relevant heating at lower concentrations than non-DNA-encased MWNTs. These lower concentrations are more likely to be achieved *in vivo* and are expected to be less toxic. Statistical analysis of the data revealed that heating of the DNA-encased MWNTs solutions was significantly greater than what occurred for the non-DNA-encased MWNTs over a broad range of times, power levels, and concentrations. The vast majority of comparisons had p-values less than 0.01 with many less than 0.001 (Supporting Information Table 1).

The linear time- and power-dependent solution ($r^2 > 0.95$, Supporting Information Table 2) heating for a given concentration of DNA-encased MWNTs is informative for identifying conditions suitable for biologically relevant heating depending on the conditions that can be achieved *in vivo*. For example, a 5 °C temperature increase can be obtained by irradiating a 5 μg/mL DNA-encased MWNT solution at 2 W for 69 s. This same temperature increase can be achieved with a 10 μg/mL DNA-encased MWNT solution for 41 s, also at 2 W irradiating power. Alternatively, a 5 °C temperature increase was achieved upon irradiating a 5 μg/mL DNA-encased MWNT solution at 4 W for 30 s. The non-DNA-encased MWNTs require greater irradiating power levels, longer duration irradiating times, or higher MWNT concentrations relative to the DNA-encased MWNTs (Supporting Information Figure S4).

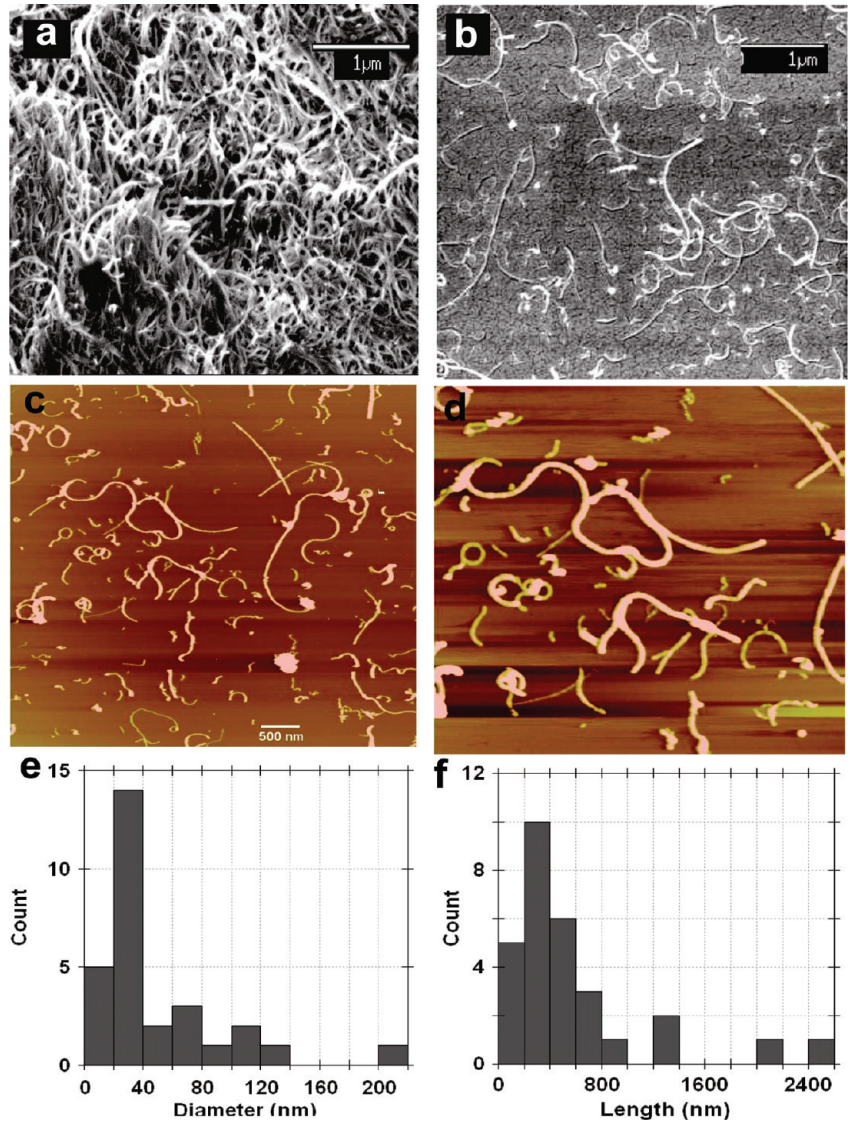

Figure 2. SEM images for (a) non-DNA-encased MWNTs and (b) DNA-encased MWNTs. Upon DNA-encasement, the MWNTs are well-dispersed with few aggregates observed. AFM images (c,d) show well-dispersed DNA-encased MWNTs and also clearly show the curvature of MWNTs. Regions of MWNT broadening are likely sites of DNA localization. The diameter (determined from the height of the AFM images) and length distribution of DNA-encased MWNTs is shown in panels e and f.

Thermal Ablation of PC3 Xenografts. The selective eradication of tumor tissue as a result of localized hyperthermia is an important objective in cancer treatment. In

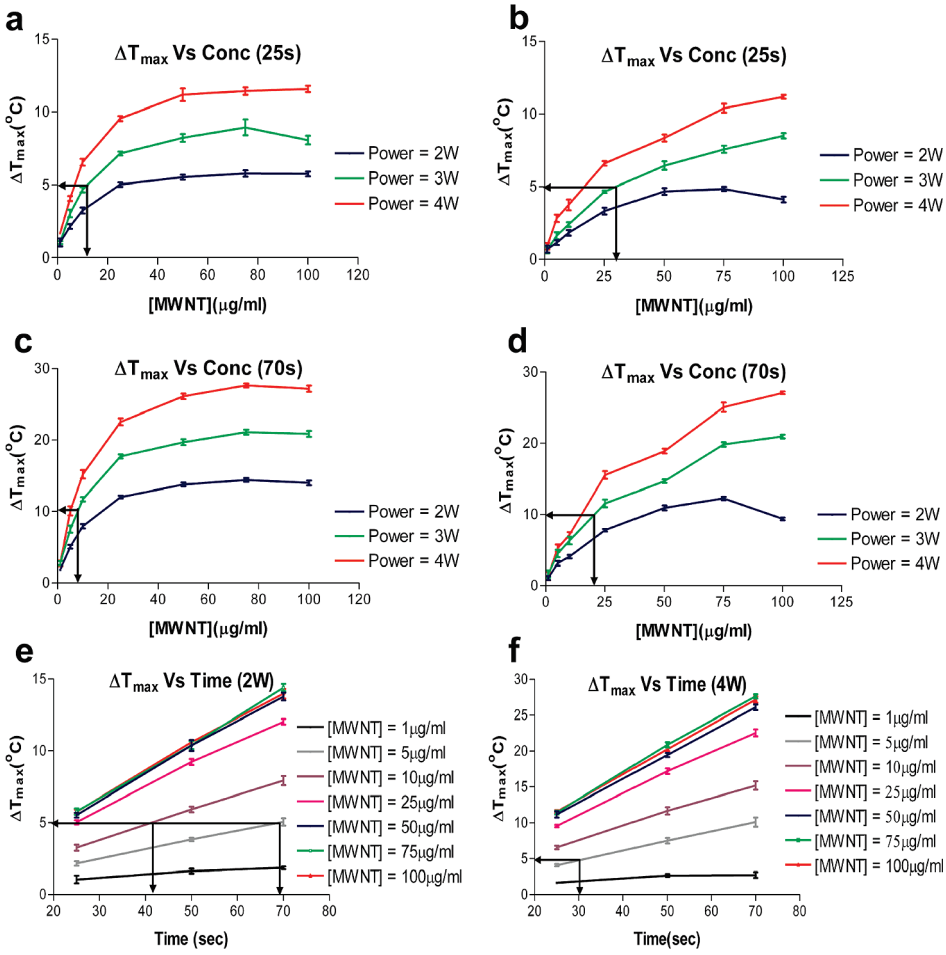

Figure 3. Representative plots for *in vitro* heating experiments with DNA-encased MWNTs. (a−d) Concentration-dependent heating of DNA-encased (a,c) and non-DNA-encased (b,d) MWNTs. The MWNT concentration required for a 5 °C increase in solution temperature upon 3 W irradiation for 25 s is indicated by horizontal and vertical arrows for DNA-encased MWNTs and for non-DNA-encased MWNTs in panels a and b, respectively. Similarly, arrows denote the concentrations required for a 10 °C temperature increase upon 3 W irradiation for 70 s in (c) DNA-encased MWNTS and (d) non-DNA-encased MWNTs. (e,f) Range of conditions suitable for a 5 °C temperature increase upon irradiation of DNA-encased MWNTs.

this study, DNA-encased MWNTs (100 μL of a 500 μg/mL solution) were injected directly into subcutaneous human tumor xenografts formed from PC3 (human prostate cancer) cells. Tumors were formed bilaterally, and treatment was initiated when tumor volumes were approximately 225 mm^3. There was no difference in tumor volumes among the four treatment groups at baseline: (1) MWNT + laser; (2) laser-only; (3) MWNT-only; (4) no treatment ($p > 0.90$). The treatment groups consisted of both left and right flank tumors from a total of 12 mice.

For the MWNT + laser treatment group (Figure 4b, top row), the right flank tumor for each of eight mice was selectively irradiated at 1064 nm for 70 s with a quasi-CW-YAG nIR laser system 1.5 h following intratumoral injection of the DNA-encased MWNT solution. The location of the DNA-encased MWNTs following intratumoral injection was readily evident by the bluish-gray color at the site of injection. For the laser-only group (Figure 4b, top row), the same eight animals that were selectively irradiated on the right flank tumor for the MWNT + laser group were also selectively irradiated on the left flank tumor. The left-flank tumor, however, received an intratumoral injection of sterile water and not DNA-encased MWNTs. The right flank tumors for four other mice were injected with DNA-encased MWNTs, but the right-flank tumors for these mice were not irradiated with a laser (MWNT-only group (Figure 4b, bottom row)). The left flank tumor for these four mice received neither laser irradiation nor MWNT injection (no treatment group (Figure 4b, bottom row)). The results are displayed in Figure 4. Of the four treatment groups (MWNT + laser, MWNT-only, laser-only, no treatment) only those tumors that received both an intratumoral injection of DNA-encased MWNTs and were subject to laser irradiation underwent a regression in tumor size. The tumors in the MWNT + laser group were all completely eradicated by day 6 following the single treatment (Figure 4).k

Tumors that received both an intratumoral injection of DNA-encased MWNTs and irradiation with a nIR laser displayed a minor surface burn (Figure 4). An antibiotic ointment was applied to the burned area and a scab formed over the burn. The scab fell off each of the tumors within 2−3 days of the lasing procedure, and the area that had been occupied by the tumor completely healed (Figure 4a) over for all eight of the animals treated. In no case, was there any evidence of tumor regrowth nor was there any evidence of long-term damage to skin. The results indicate that DNA-encased MWNTs are useful for the selective thermal eradication of malignant or hyperproliferative tissue and that this can be accomplished without any long-term damage to adjacent normal tissue.

Statistical analysis of the tumor volume data revealed that the mean tumor size for the MWNT + laser group diverged from the mean values for the other three groups (laser-only; MWNT-only; no treatment) beginning on day 6 and persisting until the end of the study. For example, comparison of the MWNT + laser

to MWNT-only showed a statistical significance beginning on day 6 ($p = 0.0109$) that increased in significance at later time points ($p < 0.001$ by day 14 and <0.0001 by day 17 and all later days). The MWNT + laser group showed similar statistical significance relative to the laser-only group ($p = 0.002$ at day 6 and $p < 0.0001$ beginning on day 10 and persisting through all later days in the study) and the no treatment group ($p = 0.014$ by day 6 and $p < 0.0001$ beginning on day 17 and persisting through all later days). The three control groups (MWNT-only, laser-only, no treatment) did not show a statistically significant difference in tumor volume at any time during the study ($p > 0.18$ for all comparisons and MWNT-only *vs* no treatment, $p = 0.6094$ at day 30). Thus, the effectiveness of treatment requires both the presence of MWNTs and laser irradiation.

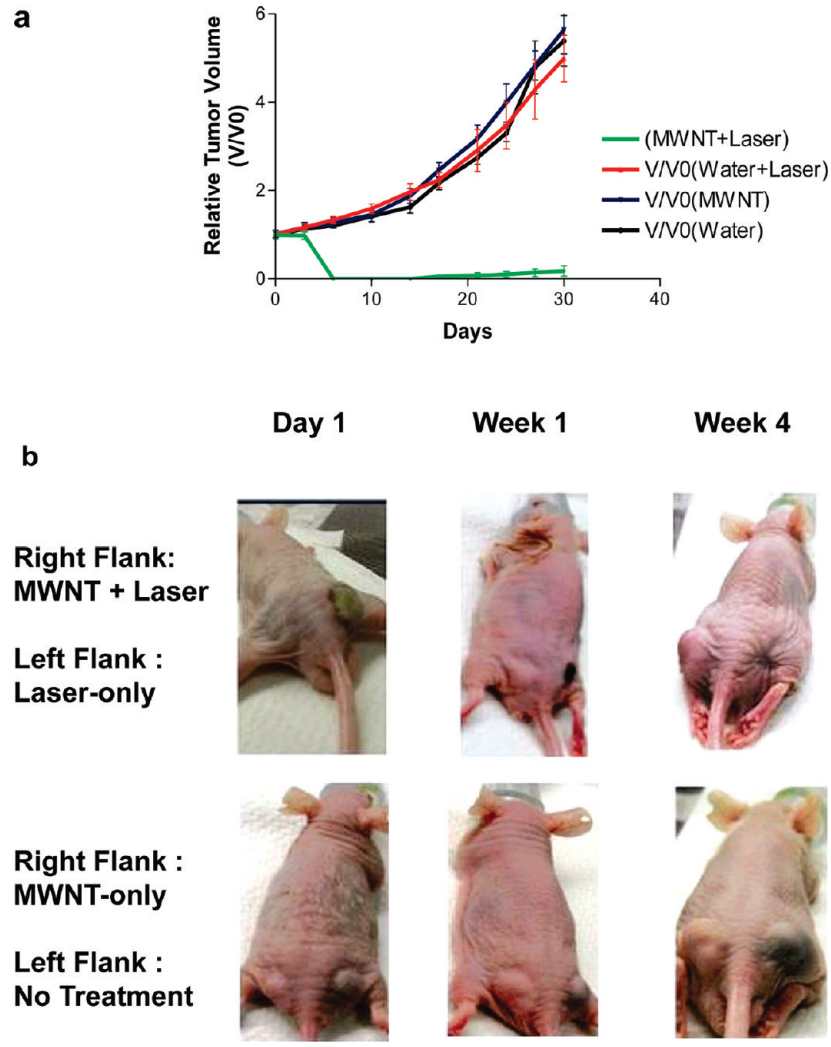

Figure 4. (a) Plot of the relative volume for the four tumor groups evaluated in the *in vivo* study. Initial tumor volumes were approximately 225 mm^3 and there was no significant difference in tumor volumes among the four groups at baseline. The tumors that were injected with DNA-encased MWNTs and irradiated with a nIR laser at 1064 nm were completely eradicated within six days following treatment for all eight animals. The region where the tumor had been was completely healed over by day 24. The tumor groups that received MWNTs-only, laser irradiation only, or no treatment grew at similar rates to one another throughout the study. (b) (top) Photographs from one animal whose right flank tumor was treated with both MWNTs and irradiated with a nIR laser at day 1, week 2, and week 4 following treatment; (bottom) photographs from one animal whose right flank tumor was treated with MWNTs-only at the same time points.

DISCUSSION

Modest temperature increases of 3−5 °C are sufficient to cause protein denaturation and subsequently cell death.[3,4] The present study demonstrates that DNA-encasement of MWNTs increases heat production 2- to 3-fold relative to non-DNA-encased MWNTs. This increased efficiency in heat production occurs over a wide range of MWNT concentrations and irradiation times and a moderate range of power levels. Importantly, the time-dependent increase in temperature for both DNA-encased MWNTs and non-DNA-encased MWNTs was linear under all conditions evaluated (Supporting Information Table 2). This finding indicates that DNA-encased MWNTs do not become saturated in any manner by continuous laser irradiation over the limited range of power levels evaluated. Rather, the optical transitions responsible for transduction of laser radiation into thermal energy may be excited continuously over the second-minute time scale without any reduction in heat generation. Thus, irradiation of a lower concentration of DNA-encased MWNTs for a longer time period resulted in as much heat as irradiation of a higher concentration for less time. These findings may be particularly significant under conditions where DNA-encased MWNTs are present at relatively low concentrations, as is likely to occur *in vivo* following i.v. administration.

Decreased aggregation is the likely origin of the increased heating from DNA-encased MWNTs relative to non-DNA-encased MWNTs. SEM and AFM images clearly show that DNA-encased MWNTs are well-dispersed while non-DNA-encased MWNTs form aggregates. Recent studies with SWNTs reveal even covalently derivatized SWNTs form bundles that constitute the active drug delivery system *in vivo*.[21] DNA may be particularly adept at disrupting nanotube aggregates because the curvature of the nanotube must match the curvature of DNA for maximal binding affinity.[14−18] Hence, while chemical dispersants such as Kentera or polyethylene glycol likely bind and confer aqueous solubility to nanotube bundles as well as to single nanotubes, DNA binding likely favors complex formation with single nanotubes as was observed in AFM and SEM images.

Toxicity concerns represent a major obstacle to the use of nanoparticles, including MWNTs, for thermal ab-

lation and drug delivery applications for cancer treatment. Thus, strategies that minimize the amount of nanoparticle required to elicit the desired biological response are important to employ at the earliest possible stage of therapeutic development. The present studies demonstrate that DNA-encasement increases heating efficiency by MWNTs. This increased heating efficiency is expected to reduce the amount of material required for an *in vivo* response. The present studies also demonstrate that for a given MWNT concentration, the required laser power could be decreased by increasing the irradiation time producing the same amount of heat while reducing damage to normal surrounding tissue *in vivo*. The present xenograft ablation study clearly demonstrates that DNA-encased MWNTs are highly efficient for *in vivo* thermal ablation. Further, DNA is a biocompatible material and its use does not impose additional risk factors for therapeutic development, such as increased immunogenicity. The high aqueous solubility of DNA-encased MWNTs also reduces the risk for aggregate formation *in vivo* that may result in adverse biological consequences.

CONCLUSIONS

There is considerable interest in the use of nanotechnology for cancer diagnosis and treatment with projected applications in drug delivery, imaging, and other areas.[11,22,23] The present study has demonstrated that DNA-encasement of MWNTs results in well-dispersed, single MWNTs that are soluble in water[7,15,24] and that display enhanced heat production efficiency relative to non-DNA-encased MWNTs. Previous studies have demonstrated that SWNTs that have been solubilized by either DNA-encasement or with PEG may be excited upon irradiation with nIR to release heat sufficient for lethality toward cancer cells in tissue culture.[7] In the present study, we have demonstrated that the conversion of nIR irradiation to heat by DNA-encased MWNTs is linear with respect to both power and time indicating that control of these parameters can be exercised to provide the desired selectivity of cell kill without damaging surrounding normal tissue. Further, we have demonstrated that DNA-encased MWNTs can be used for the selective and complete eradication of malignant tissue *in vivo*.

METHODS

Functionalization and Solubilization of MWNTs. Raw, carbon vapor deposition (CVD) MWNTs (0.05 mg/mL) were sonicated in a 4 μM (0.05 mg/mL) aqueous solution of single-stranded DNA (ssDNA; *e.g.*, $d(GT)_{40}$) at 20 °C for 50 min using a bath sonicator to yield a solution of MWNTs noncovalently associated with ssDNA (DNA-encased MWNTs). The mixture was maintained at room temperature overnight followed by centrifugation at 5000*g* for 60 min to pellet MWNT aggregates and any insoluble material. The resulting translucent supernatant consisting of DNA-encased MWNTs was filtered through a 100-kDa molecular weight cutoff (MWCO) filter (Millipore) and extensively washed with 15 mL of dH_2O to remove any unbound ssDNA. The filtration and washing steps were repeated 10 times and the efficiency of removal for free DNA was confirmed by no detectable absorbance of the final filtrates at 260 nm. The concentration of MWNT solution was determined by optical absorbance from a pre-established standard curve at 808 nm obtained using a DU800 UV−vis spectrophotometer (Beckman Coulter). The fluorescently labeled MWNT−DNA complex was prepared in an identical manner as for the nonfluorescent complex except that the ssDNA was fluorescently labeled at the 5′ terminus with FAM (Glenn Research).

Microscopic Characterization of DNA-Functionalized MWNT. AFM images were acquired under ambient conditions using a Nanoscope IIIA (Veeco Instruments, Plainview, NY) in tapping mode using silicon cantilevers (Nanosensor, type PPP-NCLR-W, force constant k = 21−98 N/m, NanoAndMore, Lady's Island, SC). Surfaces for AFM imaging were prepared by depositing 50 mM $MgCl_2$ onto freshly cleaved ruby muscovite mica surface (Paramount Corporation, NY) and allowed to dry in air. The mica surface was thoroughly rinsed with deionized water (Milli-Q Watersystem, Millipore Corp. Bedford, MA) to remove excess salt, and then dried using a gentle stream of nitrogen gas. A 20 μL drop of DNA−MWNT solution (5 μg/mL) was deposited on the substrate and air-dried. The length and diameter of the tubes was analyzed using standard Nanoscope software (version 6.13).

For scanning electron microscopy (SEM), freshly cleaved mica was treated with 100 mM $MgCl_2$ and washed thoroughly with distilled water to remove excess salt. A 5 μL drop of 25 μg/mL MWNT:DNA solution was then evenly dispersed on the mica surface and allowed to dry. The mica with dried MWNT:DNA complex was then pasted onto a stainless steel stub using silver paint. The mica surface on the stub was then sputter-coated with a very thin layer of gold−palladium mixture followed by drying. SEM images were obtained using a JEOL (JSM-6330F) field emission scanning electron microscope under high vacuum conditions using secondary electron emission mode at a working distance of 10 mm, a 12 μA probe current, and an accelerating voltage of 2.00 kV.

Spectroscopic Characterization of DNA-Functionalized MWNT. Raman spectra were acquired using a Deltanu Advantage 532 Raman spectrometer. The region from 3400−200 cm^{-1} was scanned at 532 nm excitation. Raman spectra of non-DNA complexed MWNT were obtained by placing a dry powder sample of MWNT in a capillary glass tube while Raman spectra of DNA-encased MWNTs were obtained in aqueous solution using a glass cuvette.

***In Vitro* Heating of DNA-Encased MWNTs.** The heat emitted following near-infrared (nIR) irradiation of aqueous solutions of DNA-encased MWNTs and MWNTs that had not been solubilized with DNA were evaluated by measuring the change in temperature for the aqueous solution using a digital thermometer. The 1 mL MWNT solutions were prepared at seven concentrations (1−100 μg/mL) and placed in sealed nIR-transparent glass cuvettes fitted with a microtemperature probe in the solution. Each sample was then irradiated at 1064 nm using a nIR quasi-CW-YAG laser system at a fixed power (2, 3, or 4 W/cm^2) for a fixed duration (30, 50, or 70 s). The initial temperature of each solution was recorded prior to irradiation and maximal temperature was recorded postirradiation. Temperature was monitored using a digital, continuous, temperature monitoring system. Multiway analysis of variance (ANOVA) models were fit to compare the measured temperature increases for samples of DNA-encased MWNTs and non-DNA MWNTs. In addition to the "treatment" factor (DNA-encased MWNTs *versus* non-DNA encased MWNTs) three other factors were examined in these models: time, concentration, and power. Interactions between the treatment variables and the three factors were also examined and if they were found to be significant, ANOVA models were refit stratified by the variables (time, concentration, and/or power) that had significant interactions with treatment. All models were fit using SAS version 9.1.

***In Vivo* Thermal Ablation with DNA-Encased MWNTs.** All animal experiments were performed under the protocol approved by the ani-

mal care committee of Wake Forest University Baptist Medical Center. Tumor xenografts were generated by subcutaneous injection of 3×10^6 PC3 cells suspended in 200 μL of 1:1 PBS/Matrigel in both flanks of 12 male nude mice. Mice were used for experimental procedures 2 weeks following inoculation with tumor cells, after tumor size had reached 200−250 mm^3. Each of the 12 mice were treated with 100 μL of 500 μg/mL solution of DNA-encased MWNTs injected into the right-flank tumor and 100 μL of sterile water injected into the left-flank tumor. After 1.5 h, the tumors on both flanks of 8 mice were irradiated using a nIR quasi-CW-YAG laser beam pulses with 5 s on and 3 s off for a total exposure time of 70 s at the power level of 2.5 W/cm^2. The remaining four mice were treated identically but were not exposed to the laser. The tumor sizes were measured using a caliper every third day and photographs of tumors were taken once per week. The tumor volumes were calculated using the formula $xy^2\pi/6$ (where x and y are the long and short diameters of the tumor, respectively). The tumors were analyzed as four independent groups: (1) MWNT + laser; (2) laser-only; (3) MWNT-only; (4) no treatment. Repeated measures mixed models were fit to compare tumor volumes between groups. In these models, animals were treated as random effects and group (4-levels) and time (days) were treated as fixed effects. The group by time interaction was examined to determine whether the rate of change in tumor volume differed over time among the four groups. All analyses were performed SAS 9.1.

Acknowledgment. The authors would like to acknowledge support from NIH-NCI CA102532 (W.H.G.), 2P30 CA12197-25, T32 CA05964 (E.G.), and the North Carolina Biotechnology Center. The authors are grateful to R. Noftle (WFU Chemistry) for help with Raman spectroscopy and to K. Bonin (WFU Physics) for help with fluorescence emission experiments.

Supporting Information Available: Figures summarizing the fluorescence quenching studies, detailed AFM analysis of DNA-encased MWNTs, and *in vitro* heating of DNA-encased MWNTs. This material is available free of charge *via* the Internet at http://pubs.acs.org.

REFERENCES AND NOTES

1. Lencioni, R.; Crocetti, L.; Cioni, R.; Suh, R.; Glenn, D.; Regge, D.; Helmberger, T.; Gillams, A. R.; Frilling, A.; Ambrogi, M.; Bartolozzi, C.; *et al.* Response to Radiofrequency Ablation of Pulmonary Tumours: A Prospective, Intention-to-Treat, Multicentre Clinical Trial (The Rapture Study). *Lancet. Oncol.* **2008**, *9*, 621–628.
2. Jindal, G.; Friedman, M.; Locklin, J.; Wood, B. J. Palliative radiofrequency ablation for recurrent prostate cancer. *Cardiovasc. Intervent. Radiol.* **2006**, *29*, 482–485.
3. He, X.; Wolkers, W. F.; Crowe, J. H.; Swanlund, D. J.; Bischof, J. C. *In Situ* Thermal Denaturation of Proteins in Dunning AT-1 Prostate Cancer Cells: Implication for Hyperthermic Cell Injury. *Ann. Biomed. Eng.* **2004**, *32*, 1384–1398.
4. Huang, X.; Jain, P. K.; El-Sayed, I. H.; El-Sayed, M. A. Determination of the Minimum Temperature Required for Selective Photothermal Destruction of Cancer Cells with the Use of Immunotargeted Gold Nanoparticles. *Photochem. Photobiol.* **2006**, *82*, 412–417.
5. Liang, P.; Wang, Y. Microwave Ablation of Hepatocellular Carcinoma. *Oncology* **2007**, *72*, 124–131.
6. Chakravarty, P.; Marches, R.; Zimmerman, N. S.; Swafford, A. D.; Bajaj, P.; Musselman, I. H.; Pantano, P.; Draper, R. K.; Vitetta, E. S. Thermal Ablation of Tumor Cells with Antibody-Functionalized Single-Walled Carbon Nanotubes. *Proc. Natl. Acad. Sci. U.S.A.* **2008**, *105*, 8697–8702.
7. Kam, N.; O Connell, M.; Wisdom, J.; Dai, H. Carbon Nanotubes As Multifunctional Biological Transporters and near-Infrared Agents for Selective Cancer Cell Destruction. *Proc. Natl. Acad. Sci. U.S.A.* **2005**, *102*, 11600–11605.
8. Lapotko, D.; Lukianova, E.; Potapnev, M.; Aleinikova, O.; Oraevsky, A. Method of Laser Activated Nano-Thermolysis for Elimination of Tumor Cells. *Cancer Lett.* **2006**, *239*, 36–45.
9. Carlson, L. J.; Krauss, T. D. Photophysics of Individual Single-Walled Carbon Nanotubes. *Acc. Chem. Res.* **2008**, *41*, 235–243.
10. Levy-Nissenbaum, E.; Radovic-Moreno, A. F.; Wang, A. Z.; Langer, R.; Farokhzad, O. C. Nanotechnology and Aptamers: Applications in Drug Delivery. *Trends Biotechnol.* **2008**, *26*, 442–449.
11. Welsher, K.; Liu, Z.; Daranciang, D.; Dai, H. Selective Probing and Imaging of Cells with Single Walled Carbon Nanotubes as near-Infrared Fluorescent Molecules. *Nano Lett.* **2008**, *8*, 586–590.
12. Dorin Boldor, N. M. G.; William, T. Monroe; Jason, H.; Palmer, Zhongrui Li; Alexandru, S. Biris. Temperature Measurement of Carbon Nanotubes Using Infrared Thermography. *Chem. Mater.* **2008**, *20*, 4011–4016.
13. Shvartzman-Cohen, R.; Florent, M.; Goldfarb, D.; Szleifer, I.; Yerushalmi-Rozen, R. Aggregation and Self-Assembly of Amphiphilic Block Copolymers in Aqueous Dispersions of Carbon Nanotubes. *Langmuir* **2008**, *24*, 4625–4632.
14. Helen Cathcart, S. Q.; Valeria, N; John, M. K.; Werner, J. B; Jonathan, N. C. Spontaneous Debundling of Single-Walled Carbon Nanotubes in DNA-Based Dispersions. *J. Phys. Chem. C* **2007**, *111*, 66–74.
15. Zheng, M.; Jagota, A.; Semke, E. D.; Diner, B. A.; McLean, R. S.; Lustig, S. R.; Richardson, R. E.; Tassi, N. G. DNA-Assisted Dispersion and Separation of Carbon Nanotubes. *Nat. Mater.* **2003**, *2*, 338–342.
16. Hughes, M. E.; Brandin, E.; Golovchenko, J. A. Optical Absorption of DNA-Carbon Nanotube Structures. *Nano Lett.* **2007**, *7*, 1191–1194.
17. Johnson, R. R.; Johnson, A. T.; Klein, M. L. Probing the structure of DNA-Carbon Nanotube Hybrids with Molecular Dynamics. *Nano Lett.* **2008**, *8*, 69–75.
18. Bhattarai, S. R.; Santosh, A.; C, R. B. K.; Narayan, B.; Hwang, P. H.; Yi, H. K.; Kim, H. Y. Carbon Nanotube−Hydroxyapatite Nanocomposite for DNA Complexation. *Mater. Sci. Eng. C* **2008**, *28*, 64–69.
19. Jinno, M.; Andoa, Y.; Bandowa, S.; Fanb, J.; Yudasakab, M.; Iijimaa, S. Raman Scattering Study for Heat-Treated Carbon Nanotubes: The Origin of ≈1855 cm^{-1} Raman Band. *Chem. Phys. Lett.* **2006**, *418*, 109–114.
20. Han, J.; Anantram, M. P.; Jaffe, R. L.; Kong, J.; Dai, H. Observation and Modeling of Single-Wall Carbon Nanotube Bend Junctions. *Phys. Rev. B* **1998**, *57*, 14983–14989.
21. Bhirde, A. A.; Patel, V.; Gavard, J.; Zhang, G.; Sousa, A. A.; Masedunskas, A.; Leapman, R. D.; Weigert, R.; Gutkind, J. S.; Rusling, J. F. Targeted Killing of Cancer Cells *in Vivo* and *in Vitro* with EGF-Directed Carbon Nanotube-Based Drug Delivery. *ACS Nano* **2009**, *3*, 307–316.
22. De la Zerda, A.; Zavaleta, C.; Keren, S.; Vaithilingam, S.; Bodapati, S.; Liu, Z.; Levi, J.; Smith, B. R.; Ma, T. J.; Oralkan, O.; Cheng, Z.; Chen, X.; Dai, H.; Khuri-Yakub, B. T.; Gambhir, S. S. Carbon Nanotubes As Photoacoustic Molecular Imaging Agents in Living Mice. *Nat. Nanotechnol.* **2008**, *3*, 557–562.
23. Liu, Z.; Chen, K.; Davis, C.; Sherlock, S.; Cao, Q.; Chen, X.; Dai, H. Drug Delivery with Carbon Nanotubes for *in Vivo* Cancer Treatment. *Cancer Res.* **2008**, *68*, 6652–6660.
24. Vogel, S. R.; Kappes, M. M.; Hennrich, F.; Richert, C. An Unexpected New Optimum in the Structure Space of DNA Solubilizing Single-Walled Carbon Nanotubes. *Chemistry* **2007**, *13*, 1815–1820.